haematologica
Journal of The Ferrata Storti Foundation

NCOA4-mediated ferritinophagy in macrophages is crucial to sustain erythropoiesis in mice

by Antonella Nai, Maria Rosa Lidonnici, Giorgia Federico, Mariateresa Pettinato, Violante Olivari, Federica Carrillo, Simonetta Geninatti Crich, Giuliana Ferrari, Clara Camaschella, Laura Silvestri, and Francesca Carlomagno

Haematologica 2020 [Epub ahead of print]

Citation: Antonella Nai, Maria Rosa Lidonnici, Giorgia Federico, Mariateresa Pettinato, Violante Olivari, Federica Carrillo, Simonetta Geninatti Crich, Giuliana Ferrari, Clara Camaschella, Laura Silvestri, and Francesca Carlomagno. NCOA4-mediated ferritinophagy in macrophages is crucial to sustain erythropoiesis in mice.
Haematologica. 2020; 105:xxx
doi:10.3324/haematol.2019.241232

NCOA4-mediated ferritinophagy in macrophages is crucial to sustain erythropoiesis in mice

Antonella Nai[1,2], Maria Rosa Lidonnici[3], Giorgia Federico[4], Mariateresa Pettinato[1,2], Violante Olivari[1], Federica Carrillo[4], Simonetta Geninatti Crich[5], Giuliana Ferrari[2,3], Clara Camaschella[1], Laura Silvestri[1,2]*, Francesca Carlomagno[4]*

[1] Division of Genetics and Cell Biology, San Raffaele Scientific Institute, Milan, Italy
[2] Vita-Salute San Raffaele University, Milan, Italy
[3] SR-TIGET, San Raffaele Scientific Institute, Milan, Italy
[4] Department of Molecular Medicine and Medicine Biotechnology (DMMBM), University of Naples Federico II, Naples, Italy - Institute of Endocrinology and Experimental Oncology (IEOS), CNR, Naples, Italy
[5] Department of Molecular Biotechnology and Health Sciences, University of Turin, Turin, Italy

* LS and FrC contributed equally to this work

Running Title: Macrophage ferritinophagy supports erythropoiesis

Corresponding Authors:

Francesca Carlomagno
University of Naples Federico II, DMMBM
Via Pansini 5
80131 Naples, Italy
Phone: +390815455561
E-mail: francesca.carlomagno@unina.it

And

Laura Silvestri
San Raffaele Scientific Institute
Via Olgettina, 58
20132 Milan, Italy
Phone: +390226436889
E-mail: silvestri.laura@hsr.it

Text word count: 3896

Abstract word count: 237

Number of Figures: 6

Number of Tables: 1

Number of References: 28

ACKNOWLEDGEMENTS

This paper was supported by EHA Josè Carreras Non-Clinical Junior Research Fellowship to AN, AIRC grant IG 20793 and POR Campania FESR 2014-2020 “SATIN” grant to FrC.

Abstract

The Nuclear Receptor Coactivator 4 (NCOA4) promotes ferritin degradation and *Ncoa4-ko* mice in C57BL/6 background show microcytosis and mild anemia, aggravated by iron deficiency. To understand tissue specific contribution of NCOA4-mediated ferritinophagy we explored the effect of *Ncoa4* genetic ablation in the iron-rich strain Sv129/J. Increased body iron content protects mice from anemia and, in basal conditions, Sv129/J *Ncoa4-ko* mice show only microcytosis; nevertheless, when fed a low-iron diet they develop a more severe anemia compared to wild-type animals. Reciprocal bone marrow (BM) transplantation from wild-type donors into *Ncoa4-ko* and from *Ncoa4-ko* into wild-type mice revealed that microcytosis and susceptibility to iron deficiency anemia depend on BM-derived cells. Erythropoiesis reconstitution with RBC count and hemoglobin normalization occurred at the same rate in transplanted animals independently of the genotype. Importantly, NCOA4 loss did not affect terminal erythropoiesis in iron deficiency, both in total and specific BM *Ncoa4-ko* animals compared to controls. On the contrary, upon a low iron diet, spleen from wild-type animals with *Ncoa4-ko* BM displayed marked iron retention compared to (wild-type BM) controls, indicating defective macrophage iron release in the former. Thus, EPO administration failed to mobilize iron from stores in *Ncoa4-ko* animals. Furthermore, *Ncoa4* inactivation in thalassemic mice did not worsen the hematological phenotype. Overall our data reveal a major role for NCOA4-mediated ferritinophagy in macrophages to favor iron release for erythropoiesis, especially in iron deficiency.

INTRODUCTION

The Nuclear Receptor Coactivator 4 (NCOA4), originally identified as an androgen receptor interactor(1), is a novel player in iron metabolism contributing to cell and systemic iron homeostasis regulation. NCOA4 acts as a cargo receptor that promotes “ferritinophagy”, the selective autophagy-mediated degradation of the iron storage protein ferritin(2, 3). This process is induced in conditions of iron deficiency (ID) to facilitate iron recovery from intracellular stores(4, 5).

As expected, inactivation of *NCOA4* increases cell ferritin aggregates(2-4) and C57BL/6 *Ncoa4-ko* mice show ferritin and iron accumulation in several organs, in particular splenic macrophages(3, 6). In addition, they display a mild microcytic anemia and develop a more severe anemia than wild-type (wt) when fed an ID diet(6). Whether this phenotype is due to an intrinsic defect of erythroid cells or to store iron retention because of impaired ferritin degradation due to *Ncoa4* inactivation is a matter of investigation.

Some evidence argues in favor of an intrinsic erythroid function for NCOA4. First, *NCOA4* is expressed at high levels in maturing orthocromatic erythroblasts(7); second, *in vitro*(4, 8) and *ex vivo* data(9) suggest that NCOA4 is required for erythroid cells differentiation and hemoglobinization, modulating iron incorporation into heme. An erythropoietic role for NCOA4 was suggested also *in vivo* in zebrafish embryos treated with morpholinos to *Ncoa4*(4). A moderate-severe anemia was observed in *Ncoa4-ko* mice at birth, mostly rescued in adult animals(9, 10). Despite all these findings

suggest a role for NCOA4 in erythropoiesis, a formal proof that anemia of adult *Ncoa4-ko* mice is due to loss of protein activity in erythroid cells is still lacking. Recent data(10) point toward both an autonomous and non-autonomous effect of NCOA4 in erythropoiesis. The Authors generated a conditional tamoxifen-induced total *Ncoa4-ko* model and a tissue specific one [through the expression of CRE-recombinase under the control of Erythropoietin Receptor (EPOR) promoter in *Ncoa4-floxed* transgenic animals]. However, both tamoxifen-induced toxic effects on red blood cells(11) and non erythroid-restricted expression of EPOR(12) still leave the question open.

In order to clarify the *in vivo* function of NCOA4, its role in erythropoiesis and to identify the cell type mostly affected by *Ncoa4* deficiency *in vivo* we used different approaches. First we generated *Ncoa4-ko* mice on the iron-rich Sv129/J strain and analyzed the animals in basal status and after different challenges. Then, we performed reciprocal bone marrow transplantation (BMT) of wt and *Ncoa4*-ko BM respectively in *Ncoa4-ko* and wt mice. Finally, we crossed *Ncoa4*-ko with $Hbb^{th3/+}$ mice, a model of transfusion-independent β-thalassemia. We proved that reduced iron release by macrophages is the principal driver of anemia in *Ncoa4-ko* animals and excluded a relevant role for NCOA4 in erythroid cells *in vivo*.

METHODS

Mouse models and bone marrow transplantation

Ncoa4-ko mice on Sv129/J background were generated as described in (6)

and in supplemental materials. Wild-type littermates were used as controls in all the experiments. When not specified otherwise, mice were fed a standard diet containing 280 mg/kg of carbonyl iron.

Blood was collected by tail vein puncture for complete blood count (CBC) at 3, 5, 8 and 9 months of age. Mice were sacrificed when 3 or 9-month-old and blood collected for transferrin saturation (TS) determination. Liver, spleen and kidneys were weighed, dissected and snap-frozen for RNA and protein analysis or dried for iron quantification or processed for FACS analysis. BM cells were harvested and processed for methylcellulose assay, flow cytometry or RNA analysis. Duodenum was washed and formalin-fixed for Perl's staining.

BMT was performed as described in (13) and in supplemental materials. CBC was evaluated monthly. At sacrifice animals were analyzed as above.

A subset of *Ncoa4-ko* mice was crossed to C57BL/6N $Hbb^{th3/+}$ animals(14) (Jackson Laboratories, Bar Harbor, ME, USA) obtaining $Ncoa4^{+/-}$ and $Ncoa4^{+/-}/Hbb^{th3/+}$ progenies on a mixed C57/129 background; these animals were back-crossed generating $Ncoa4^{-/-}/Hbb^{th3/+}$, $Ncoa4^{+/-}/Hbb^{th3/+}$ and $Hbb^{th3/+}$ mice. Blood was collected for CBC evaluation from 1, 2 and 4-month-old animals of both gender.

All mice were maintained in the San Raffaele Institute animal facility in accordance with the European Union guidelines. The study was approved by the *Institutional Animal Care and Use Committee* of San Raffaele Institute.

Treatments

For the induction of iron deficiency, *Ncoa4-ko* mice of both gender were fed an iron-deficient (ID) diet containing less than 3 mg/kg of carbonyl iron, (SAFE, Augy, France) for 6 months starting when 3-month-old. Transplanted mice were fed a standard diet for 2 months and then the ID diet until sacrificed 5 months after BMT.

For the evaluation of duodenal iron absorption, 9-month-old wt and *Ncoa4-ko* mice (of both gender) were administered 100µl of a solution containing 228.5 mg/L of the stable iron isotope ^{57}Fe (Sigma-Aldrich) by oral gavage. The animals were fasted 16 hours before ^{57}Fe administration and one hour after gavage anesthetized by Avertin i.p. (2,2,2-tribromoethanol, 250 mg/kg; Sigma-Aldrich). Blood for serum preparation was recovered via retro orbital withdrawal and mice were subsequently perfused transcardially with phosphate-buffered saline (PBS). Duodenum and liver were recovered, washed with PBS, weighed and immediately snap-frozen.

For the induction of acute erythropoietic expansion, wt and *Ncoa4-ko* mice (of both gender) were treated with a single injection of erythropoietin (EPO, 0.8UI/g) or saline as a control and sacrificed 15 hours later.

At sacrifice all animals were analyzed as described above.

Phenotypic characterization

CBC, transferrin saturation and tissue iron content determination, flow cytometry analysis, colony-forming unit assay, Perl's blue staining, inductively coupled plasma mass spectrometry, western-blot analysis and quantitative real-time PCR were performed by standard methods. See supplemental

material for details.

Statistics

Data are presented as mean ± standard error (SE). Unpaired 2-tailed Student's t-test (for normal distributions) or Mann-Whitney test (for non Gaussian distributions) were performed using GraphPad Prism 5.0 (GraphPad). $P<0.05$ was considered statistically significant.

RESULTS

Ncoa4-ko mice on Sv129/J background show microcytic red cells but not anemia

Given the significant impact of mouse strain on iron metabolism(15), we investigated the phenotype of *Ncoa4-ko* mice on Sv129/J background, a strain more iron rich than C57BL/6 (A.N. and L.S., unpublished data & (16)). For comparison with *Ncoa4-ko* C57BL/6 age-matched animals(6), complete blood cell (CBC) count was periodically determined until 9 months of age when mice were sacrificed. Differently from C57BL/6 animals, red blood cells (RBCs) count, hematocrit (not shown) and hemoglobin (Hb) levels were similar in Sv129/J *Ncoa4-ko* mice and wild-type littermates (wt). Only the erythrocytes indexes mean corpuscular volume (MCV) and mean corpuscular hemoglobin (MCH) were slightly lower (about 4.4% and 6% of reduction respectively) in mutant mice than in controls, at all ages analyzed, as occurred in the C57BL/6 strain[6] (**Figure 1A**). Bone marrow (BM) and spleen (SP) erythroid differentiation (**Figure 1B**) was similar in wt and *Ncoa4-ko* mice at 3 and 9 months of age (**Figure 1C** and data not shown). *Ncoa4-ko* BM cells

generated the same number of BFU-E and CFU-GM as wt BM cells in methylcellulose assays (**Figure 1D**). Consistent with normal Hb levels, erythropoietin (*Epo*) expression in the kidney was comparable in wt and *Ncoa4-ko* animals (**Supplemental Figure S1A**).

Overall these results show that the lack of *Ncoa4* in an iron-rich background causes only mild microcytosis without anemia, preserves normal maturation and does not impair erythroid cells clonogenic capacity, thus excluding important differentiation defects *in vivo*.

Ncoa4-ko mice have normal iron parameters but tissue iron retention in ferritin

At difference from C57BL/6 mice(6), 9-month-old Sv129/J *Ncoa4-ko* mice had transferrin saturation, serum iron levels and liver (LIC), spleen (SIC) and kidney (KIC) non-heme iron content comparable to wt mice (**Table 1**). However, iron retention is evident in duodenal sections of *Ncoa4-ko* animals (**Figure 2A**), as observed in C57BL/6 mice(6).

Duodenal iron accumulation was not due to increased expression of the iron-regulatory hormone hepcidin (*Hamp*) that was instead reduced in mutant mice (**Figure 2B**). The inhibition of *Hamp* was likely mediated by down-regulation of the BMP-SMAD pathway, as suggested by the low expression of the BMP-SMAD target gene Inhibitor of differentiation 1 (*Id1*) (**Figure 2C**). This occurred in the presence of normal expression levels of the hepcidin activators *Bmp6* and *Bmp2* and of the hepcidin inhibitor erythroferrone (*Erfe*) both in BM and spleen (**Supplemental Figure S1B-E**). Despite normal LIC, Transferrin Receptor 1 (*Tfr1*) expression, which is inversely correlated to

intracellular iron, was increased in liver of *Ncoa4-ko* mice (**Figure 2D**), in line with results obtained in *NCOA4*-depleted cells(2). *Tfr1* expression was increased also in the kidney of mutant mice (**Supplemental Figure S1F**), despite normal kidney iron content. On the other hand, liver ferritin H levels were increased, as expected because of ferritinophagy impairment (**Figure 2E**). Overall these data suggest that irrespective of normal iron concentration, *Ncoa4-ko* tissues sense a signal of iron deficiency, likely due to reduced "free" iron pool secondary to ferritin iron retention.

Ncoa4-ko mice are susceptible to iron deficiency

To characterize their capacity to release iron from the stores in chronic iron deficiency, a cohort of wt and *Ncoa4-ko* mice was challenged with an iron poor diet (ID) for 6 months starting at 3 months of age. Surprisingly this diet did not significantly affect the hematological parameters of wt mice likely because of the high body iron content of the Sv129/J strain. As C57BL/6 mice, Sv129/J *Ncoa4-ko* fed with a low-iron diet developed severe anemia, especially in the last month of diet (**Figure 3A**). BM and spleen erythropoiesis in *Ncoa4-ko* mice remained substantially comparable to wt, with similar percentage of Ter119+ cells and without evident maturation differences (**Figure 3B**). However, *Ncoa4-ko* cells isolated from ID mice generated significantly less BFU-E and CFU-GM than wt cells (**Figure 3C**), suggesting that severe iron deficiency impairs the clonogenic capacity of early progenitors cells lacking *Ncoa4*.

ID reduced the levels of circulating and tissue iron in both genotypes. After 6 months *Ncoa4-ko* mice had transferrin saturation and serum iron levels

dramatically lower than wt littermates, while LIC, SIC, KIC (**Table 1**) and Perl's staining on duodenal sections (**Supplemental Figure S2A**) were comparably decreased. These results suggest that under a prolonged chronic ID, *Ncoa4-ko* mice likely mobilize stored iron through NCOA4-independent mechanisms. Nevertheless, liver ferritin levels remain higher in *Ncoa4-ko* mice than in wt, consistent with reduced ferritin degradation (**Supplemental Figure S2B**). Liver *Hamp, Id1* and *Bmp6* expression were similarly decreased in *Ncoa4-ko* and wt mice (**Supplemental Figure S2C-E**). *Ncoa4-ko* mice showed a trend towards liver *Tfr1* increased expression (**Supplemental Figure S2F**) and a significant kidney *Tfr1* upregulation (**Supplemental Figure S2G**), despite iron content was comparable to wt mice. This is consistent with a functional iron deficiency, as observed under standard diet. The kidney *Epo* expression was higher in anemic *Ncoa4-ko* mice than in wt (**Supplemental Figure S2H**), as expected.

Overall these results suggest that in chronic iron deficiency impaired ferritinophagy decreases iron availability for erythropoiesis in *Ncoa4-ko* mice, thus causing severe anemia.

Because of the relevance of iron absorption in iron deficiency and hypoxia (17, 18), we wondered whether the lack of *Ncoa4* could also impact on duodenal iron uptake. To address this point, 9-month-old *Ncoa4-ko* and wt controls were treated with a single dose of ^{57}Fe via oral gavage (100 µl/mouse of a solution containing 228 mg/l ^{57}Fe) and sacrificed 1 hour later(19). The amount of ^{57}Fe determined via inductively coupled plasma mass spectrometry (ICP-MS) in the duodenum, serum and liver (**Supplemental Figure S3**) was

similar in wt and *Ncoa4-ko* animals, excluding that the lack of *Ncoa4* significantly impairs dietary iron uptake.

Ncoa4-k*o bone marrow reconstitutes normal erythropoiesis *in vivo

To investigate erythropoiesis of *Ncoa4-ko mice* more in depth, we used BM transplantation (BMT) to assess the capacity of *Ncoa4*-deficient hematopoietic stem cells to reconstitute erythropoiesis. BMT replaces all recipient hematopoietic lineages, spleen macrophages(20) and partially liver macrophages(21) with donor cells. Lethally irradiated *Ncoa4-ko* mice were transplanted with BM cells from wt littermates (and from *Ncoa4-ko* as controls) (**Figure 4A**). Wild-type mice were transplanted with BM cells from *Ncoa4-ko* donors (and from wt littermates as control) (**Supplemental Figure S4A**).

Two months after BMT, erythropoiesis was fully recovered in animals transplanted with both *Ncoa4-ko* and wt BM, with comparable RBC count and Hb levels (**Figure 4B** and **Supplementary Figure S4B-E**). This result disputes the impaired differentiation capacity of *Ncoa4-ko* erythroid progenitors/precursors *in vivo*.

Ncoa4-ko mice transplanted with wt BM fully corrected microcytosis with MCV reaching levels of untransplanted wt mice (**Figure 4B**). Conversely, wild-type mice transplanted with *Ncoa4-ko* BM developed a mild microcytosis, comparable to that of germ-line *Ncoa4-ko* animals (**Supplementary Figure S4B-E**).

These experiments clearly demonstrate that the microcytosis of *Ncoa4-ko* mice is due to the loss of NCOA4 exclusively in BM-derived cells, either

erythroid cells or macrophages or both. However, considering not only the normal erythropoiesis documented in *Ncoa4-ko* mice but also the ability of ko BM cells to completely reconstitute erythropoiesis in lethally irradiated animals, our conclusion is that a major defect in erythroid precursors lacking *Ncoa4* is unlikely.

Ncoa4-ko* macrophages display impaired ferritinophagy *in vivo

To better characterize ferritinophagy impairment in *Ncoa4-ko* macrophages, *Ncoa4-ko* mice reconstituted with *Ncoa4-ko* (*Ncoa4-ko*$^{ko\ BM}$) or wt BM cells (*Ncoa4-ko*$^{wt\ BM}$) were fed a low iron diet for 3 months starting 2 months after BMT. The ID diet period was shorter than the one used in germ-line animals to avoid the activation of the NCOA4-independent compensatory mechanisms of iron release observed in total *Ncoa4-ko* mice. The ID diet reduced Hb levels, MCV and MCH without affecting RBC count in both genotypes, with a trend toward a more severe effect in *Ncoa4-ko*$^{ko\ BM}$ transplanted mice (**Figure 4B**), confirm that the susceptibility to iron-deficiency of *Ncoa4-ko* mice is due to a defect in BM-derived cells. The comparable BM and spleen erythroid differentiation between the 2 genotypes (**Figure 4C**) argues against an intrinsic defect of *Ncoa4-ko* erythroid cells rather suggesting that microcytosis and increased iron deficiency susceptibility result from defective iron release by *Ncoa4-ko* macrophages.

In support of this interpretation, after 3 months of diet spleen iron content in *Ncoa4-ko*$^{ko\ BM}$ mice was higher than in controls (**Figure 4D**), consistent with a defect of *Ncoa4-ko* macrophages in releasing iron *in vivo*, despite comparable transferrin saturation (**Supplementary Figure S5A**), serum iron levels

(**Supplementary Figure S5B**) and LIC (**Figure 4E**) between the two genotypes. Splenic iron accumulation did not result from increased hepcidin levels (**Supplementary Figure S5C**), but from impaired degradation of ferritin. Indeed ferritin levels in the spleen of *Ncoa4-ko*$^{ko\ BM}$ animals persisted higher than in mice transplanted with wt cells (**Figure 4F**).

Despite comparable iron content, liver ferritin levels were higher in the *Ncoa4-ko*$^{ko\ BM}$ mice than in *Ncoa4-ko*$^{wt\ BM}$ controls (**Figure 4G**), suggesting impaired ferritin degradation also in this tissue. Being macrophages the sole hepatic cells derived, at least in part, from donor BM(21), these results further confirm the reduced ability of *Ncoa4-ko* macrophages in degrading ferritin. Limited macrophage ferritinophagy, restricting iron recycling, explains the severity of anemia in ID and supports a prevalent non-autonomous role of NCOA4 in erythropoiesis.

Ncoa4-ko mice fail to raise circulating iron levels upon acute erythropoietic expansion

Iron recycling is essential not only to compensate chronic anemia but also in response to the acute expansion of erythropoiesis as after bleeding or erythropoietin stimulation. To verify the role played by NCOA4 in response to acute increase of iron demand *in vivo,* we exploited a published protocol(22, 23), treating wt and *Ncoa4-ko* mice with a single EPO injection (8 UI/g body weight) to induce erythropoietic expansion, increased erythroferrone release(24) and inhibition of hepcidin. In normal mice, iron uptake from the diet and release from the stores are enhanced to supply erythropoiesis, resulting in a transient increase in the levels of serum iron 15 hours after EPO

administration (**Figure 5A** and (22)). At this time point no significant changes of BM erythropoiesis were observed, while the percentage of early erythroid precursors was increased in the spleen in both wt and *Ncoa4-ko* mice (**Figure 5B** and **Supplemental Figure S6A**). The induction of splenic *Erfe* was comparable in both genotypes (**Figure 5C**) and hepcidin inhibition was even stronger in mutant than in wt mice (**Figure 5D**). Despite low hepcidin levels and at difference with wt, transferrin saturation and serum iron levels were not increased in EPO-treated *Ncoa4-ko* mice (**Figure 5E**-**F**). These data indicate that the latter mice fail to mobilize iron stores in response to an acute increase of iron demand. The hypoferremia observed in the latter animals likely contributes to decrease hepcidin, suppressing the BMP-SMAD pathway, as suggested by the concomitant reduction of *Id1* mRNA, in the absence of *Bmp6* and *Bmp2* changes (**Supplementary Figure S6B-D**).

Ncoa4 deletion does not furtherly worsen anemia in thalassemic mice

To further prove the non-autonomous role of NCOA4 in erythropoiesis, we investigated the effect of *Ncoa4* heterozygous or homozygous deletion in $Hbb^{th3/+}$ animals, a model of transfusion-independent thalassemia, characterized by deficiency of β-globin chain, ineffective erythropoiesis and anemia(14). We reasoned that *Ncoa4* genetic inactivation would have worsen the erythroid phenotype of $Hbb^{th3/+}$ animals, in case NCOA4 was playing an important role in hemoglobinization of erythroid precursors, as suggested(5). To this aim, *Ncoa4-ko* mice were bred with $Hbb^{th3/+}$ animals and CBC evaluated at 1 and 2 and 4 months of age in double mutants. *Ncoa4* haploinsufficiency had no effect on anemia of $Hbb^{th3/+}$ mice at all time points

(**Figure 6**). Deletion of both *Ncoa4* alleles induced a modest, statistically significant increase of RBC count at 2 and 4 month of age (**Figure 6A**), that may result from the iron-restricted phenotype caused by reduced iron recycling, as suggested by further decreased MCV (**Figure 6C**) and MCH (**Figure 6D**) of double mutants mice compared to $Hbb^{th3/+}$ controls.

In conclusion *Ncoa4* deletion does not aggravate anemia in this model, suggesting a minor, if any, effect of NCOA4 in erythropoiesis. The stable or even slightly improved phenotype secondary to the loss of *Ncoa4* is in line with mild iron restriction, a condition described to ameliorate the thalassemic phenotype (25-27).

DISCUSSION

NCOA4-mediated ferritinophagy is essential for maintaining cell and systemic iron homeostasis(2-6, 9). Importantly, loss of NCOA4 function *in vivo* induces anemia especially in low iron conditions. Which cell type/s mostly depend on NCOA4 and ferritinophagy in order to sustain iron-dependent processes, and especially erythropoiesis, remains uncertain.

Here, by combining different experimental approaches, we dissected the tissue specific role of NCOA4 and ferritinophagy in supporting red blood cells production and show that the major function of NCOA4 is in iron recycling macrophages.

First, we demonstrate the relevance of total body iron as a modifier of the phenotype of *Ncoa4-ko* mice. Anemia is not a feature of *Ncoa4-ko* mice on

Sv129/J, a strain with higher body iron than the C57BL/6 [(16) and personal data]. Terminal erythropoiesis proceeds normally in *Ncoa4-ko* mice and BM cells isolated from both 3- and 9-month-old mice fed a standard diet generate the same number of BFU-e and CFU-GM as wt cells. However, anemia is induced more easily in *Ncoa4-ko* mice than in controls by a prolonged iron-deficient diet. Lack of anemia in iron replete conditions and increased susceptibility to anemia in iron deficiency suggest that the erythroid phenotype in *Ncoa4-ko* mice is strongly dependent on the efficacy of iron supply. Indeed, had NCOA4 been crucial in erythroid cells differentiation and hemoglobinization, anemia would have developed in *Ncoa4-ko* animals irrespective of the genetic background. Intriguingly, while NCOA4 is fundamental for providing iron in acute conditions, a prolonged (6 months) ID diet leads to a substantial splenic and hepatic iron mobilization in *Ncoa4-ko* mice, suggesting that NCOA4-independent mechanisms are likely activated in chronic conditions, although these are insufficient to prevent the development of anemia.

Second, after bone marrow transplantations *Ncoa4*-ko BM cells reconstitute normal RBC count and Hb levels in both wt and *Ncoa4-ko* recipients, with microcytosis being their only abnormality. The ability to reconstitute normal erythropoiesis and normal Hb and RBC count proves that loss of *Ncoa4 in vivo* has a limited, if any, effect on the erythroid lineage. In addition, haploinsufficiency and total *Ncoa4* ablation do not worsen anemia of a β-thalassemia mouse on a long term. In case of an autonomous erythroid role for NCOA4 one would have expected that its deletion in a context of a

constitutionally abnormal erythropoiesis would have further decreased hemoglobin levels. Our results, instead, suggest that the iron-restricted phenotype of *Ncoa4-ko* mice protects erythroid precursors from oxidative stress and improves red blood cell production, as observed by other iron restrictive approaches (25-27), although enhancing microcytosis.

The autonomous erythroid function proposed for NCOA4 in a recent publication was based on tamoxifen-inducible total *Ncoa4-ko* mice, which develop acute anemia after tamoxifen treatment(10). However, our recent finding that tamoxifen has a toxic effect on RBC production, even stronger in mice lacking *Ncoa4,* weakens the authors' conclusion(11). The same Authors also generated an erythropoietin receptor (*Epor)-Cre Ncoa4*-floxed mice in which *Ncoa4* genetic ablation was induced by Cre recombinase expressed under the control of the *Epor* promoter(10). The microcytic anemia of these animals was considered a proof of NCOA4 cell autonomous function in erythroid compartment. However, *Epor* is not exclusively expressed in the erythroid lineage but also in other cell types, including macrophages(12). This raises concerns about the erythroid specificity of the model and makes the reported findings not conclusive for a NCOA4 self-autonomous erythroid role.

It is important to note that the modest microcytosis of *Ncoa4-ko* animals was reproduced by reconstituting lethally irradiated wild-type mice with *Ncoa4-ko* BM cells, while it was completely rescued by transplanting *Ncoa4-ko* animals with wt BM-derived cells. These findings indicate that microcytosis results from the lack of NCOA4 in BM-derived cells, excluding the role of other cells e.g. the iron absorptive enterocytes, that are *ko* in *Ncoa4-ko* mice transplanted with wt donors. In agreement, *Ncoa4-ko* mice show normal

uptake and distribution of orally administered iron isotope ^{57}Fe. Although the technique is likely unable to detect subtle differences in absorption, we concluded that iron sequestration into ferritin caused by *Ncoa4* deficiency, despite inducing a condition of functional iron-deficiency, does not substantially alter the HIF-2α mediated orchestration of duodenal iron homeostasis(17, 18) *in vivo*, as recently shown in an *in vitro* cellular model in which *Ncoa4* was silenced(28).

While limiting the NCOA4 role in erythroid precursors and enterocytes, our data point to a crucial function for ferritinophagy in macrophages. *Ncoa4-ko* macrophages have impaired iron recycling capacity *in vivo,* likely secondary to their reduced ability of degrading ferritin, a defect exacerbated by acute increase of iron demand. However, this does not translate into decreased saturation of transferrin, except in conditions of acute requests, as after EPO administration. Our observation is in line with results obtained in mice with selective inactivation of the iron exporter ferroportin that develop a more severe anemia than wt controls when fed an iron-poor diet(29) because of their impaired iron export capacity. We also speculate that ferritinophagy impairment in the central nurse macrophage of the erythroblastic island might affect the iron supply to maturing erythroblasts (30), resulting in slightly microcytic red cells when circulating iron is normal and in anemia when transferrin bound iron is limited in ID.

NCOA4 is a multifunctional protein. We observed that BM cells, isolated from iron-deficient *Ncoa4-ko* mice, generate a lower number of BFU-E and CFU-GM-derived colonies compared to wt animals, indicating a role for NCOA4 in early BM progenitors. We hypothesize that in mild iron deficiency, wt

progenitors increase their rate of proliferation and DNA replication to sustain erythropoiesis and that this process likely requires NCOA4 in order to promote ferritinophagy and simultaneously control DNA replication origin activation to avoid replication stress [(31) and Federico et al, in preparation]. In agreement, a defect in the clonogenic capacity was found in cells isolated from *Ncoa4-ko* newborn mice(9), a condition characterized by high iron requests and functional iron deficiency. The clonogenic defect recovers in adult age, when iron availability increases.

All together our results demonstrate the NCOA4 crucial role in regulating iron homeostasis, in particular in response to increased iron requirements. Although a minor erythroid effect cannot be definitely excluded by all the available approaches, NCOA4 function in macrophages is the main driver of the hematological alterations observed in *Ncoa4-ko* mice.

AUTHOR CONTRIBUTIONS

A.N. designed and performed experiments, analyzed data and wrote the manuscript; M.R.L., Gio.Fed., M.P., V.O., Fe.C. and S.G.C. performed research and contributed to analyze data; Giu.Fer. contributed to data analysis and manuscript writing; C.C. contributed to the experimental design and manuscript preparation; L.S. and Fr.C. conceived the experiments and critically reviewed the paper. All Authors approved the final version of the manuscript.

DISCLOSURE OF CONFLICT OF INTERESTS

CC is an advisor of Vifor Iron Core and received honoraria from Vifor Pharma.

The other authors declare no financial conflict of interests.

REFERENCES

1. Yeh S, Chang C. Cloning and characterization of a specific coactivator, ARA70, for the androgen receptor in human prostate cells. Proc Natl Acad Sci U S A. 1996;93(11):5517-5521.
2. Mancias JD, Wang X, Gygi SP, Harper JW, Kimmelman AC. Quantitative proteomics identifies NCOA4 as the cargo receptor mediating ferritinophagy. Nature. 2014;509(7498):105-109.
3. Dowdle WE, Nyfeler B, Nagel J, et al. Selective VPS34 inhibitor blocks autophagy and uncovers a role for NCOA4 in ferritin degradation and iron homeostasis in vivo. Nat Cell Biol. 2014;16(11):1069-1079.
4. Mancias JD, Pontano Vaites L, Nissim S, et al. Ferritinophagy via NCOA4 is required for erythropoiesis and is regulated by iron dependent HERC2-mediated proteolysis. Elife. 2015;4.
5. Ryu MS, Duck KA, Philpott CC. Ferritin iron regulators, PCBP1 and NCOA4, respond to cellular iron status in developing red cells. Blood Cells Mol Dis. 2018;69:75-81.
6. Bellelli R, Federico G, Matte A, et al. NCOA4 Deficiency Impairs Systemic Iron Homeostasis. Cell Rep. 2016;14(3):411-421.
7. An X, Schulz VP, Li J, et al. Global transcriptome analyses of human and murine terminal erythroid differentiation. Blood. 2014;123(22):3466-3477.
8. Ryu MS, Zhang D, Protchenko O, Shakoury-Elizeh M, Philpott CC. PCBP1 and NCOA4 regulate erythroid iron storage and heme biosynthesis. J Clin Invest. 2017;127(5):1786-1797.
9. Gao X, Lee HY, Li W, et al. Thyroid hormone receptor beta and NCOA4 regulate terminal erythrocyte differentiation. Proc Natl Acad Sci U S A. 2017;114(38):10107-10112.
10. Santana-Codina N, Gableske S, Quiles Del Rey M, et al. NCOA4 maintains murine erythropoiesis via cell autonomous and non-autonomous mechanisms. Haematologica. 2019;104(7):1342-1354.
11. Nai A, Pettinato M, Federico G, Olivari V, Carlomagno F, Silvestri L. Tamoxifen erythroid toxicity revealed by studying the role of Nuclear Receptor Co-Activator 4 in erythropoiesis. Haematologica. 2019;104(8):e383-e384.
12. Jelkmann W, Bohlius J, Hallek M, Sytkowski AJ. The erythropoietin receptor in normal and cancer tissues. Crit Rev Oncol Hematol. 2008;67(1):39-61.
13. Nai A, Lidonnici MR, Rausa M, et al. The second transferrin receptor regulates red blood cell production in mice. Blood. 2015;125(7):1170-1179.
14. Yang B, Kirby S, Lewis J, Detloff PJ, Maeda N, Smithies O. A mouse model for beta 0-thalassemia. Proc Natl Acad Sci U S A. 1995;92(25):11608-11612.

15. Fleming RE, Holden CC, Tomatsu S, et al. Mouse strain differences determine severity of iron accumulation in Hfe knockout model of hereditary hemochromatosis. Proc Natl Acad Sci U S A. 2001;98(5):2707-2711.
16. Levy JE, Montross LK, Cohen DE, Fleming MD, Andrews NC. The C282Y mutation causing hereditary hemochromatosis does not produce a null allele. Blood. 1999;94(1):9-11.
17. Mastrogiannaki M, Matak P, Keith B, Simon MC, Vaulont S, Peyssonnaux C. HIF-2alpha, but not HIF-1alpha, promotes iron absorption in mice. J Clin Invest. 2009;119(5):1159-1166.
18. Shah YM, Matsubara T, Ito S, Yim SH, Gonzalez FJ. Intestinal hypoxia-inducible transcription factors are essential for iron absorption following iron deficiency. Cell Metab. 2009;9(2):152-164.
19. Fiorito V, Geninatti Crich S, Silengo L, Altruda F, Aime S, Tolosano E. Assessment of iron absorption in mice by ICP-MS measurements of (57)Fe levels. Eur J Nutr. 2012;51(7):783-789.
20. Kaur S, Raggatt LJ, Millard SM, et al. Self-repopulating recipient bone marrow resident macrophages promote long-term hematopoietic stem cell engraftment. Blood. 2018;132(7):735-749.
21. Beattie L, Sawtell A, Mann J, et al. Bone marrow-derived and resident liver macrophages display unique transcriptomic signatures but similar biological functions. J Hepatol. 2016;65(4):758-768.
22. Artuso I, Pettinato M, Nai A, et al. Transient decrease of serum iron after acute erythropoietin treatment contributes to hepcidin inhibition by ERFE in mice. Haematologica. 2018;104(3):e87-e90.
23. Mirciov CSG, Wilkins SJ, Hung GCC, Helman SL, Anderson GJ, Frazer DM. Circulating iron levels influence the regulation of hepcidin following stimulated erythropoiesis. Haematologica. 2018;103(10):1616-1626.
24. Kautz L, Jung G, Valore EV, Rivella S, Nemeth E, Ganz T. Identification of erythroferrone as an erythroid regulator of iron metabolism. Nat Genet. 2014;46(7):678-684.
25. Gardenghi S, Ramos P, Marongiu MF, et al. Hepcidin as a therapeutic tool to limit iron overload and improve anemia in beta-thalassemic mice. J Clin Invest. 2010;120(12):4466-4477.
26. Li H, Rybicki AC, Suzuka SM, et al. Transferrin therapy ameliorates disease in beta-thalassemic mice. Nat Med. 2010;16(2):177-182.
27. Nai A, Pagani A, Mandelli G, et al. Deletion of TMPRSS6 attenuates the phenotype in a mouse model of beta-thalassemia. Blood. 2012;119(21):5021-5029.
28. Schwartz AJ, Das NK, Ramakrishnan SK, et al. Hepatic hepcidin/intestinal HIF-2alpha axis maintains iron absorption during iron deficiency and overload. J Clin Invest. 2019;129(1):336-348.
29. Zhang Z, Zhang F, An P, et al. Ferroportin1 deficiency in mouse macrophages impairs iron homeostasis and inflammatory responses. Blood. 2011;118(7):1912-1922.
30. Nairz M, Theurl I, Swirski FK, Weiss G. "Pumping iron"-how macrophages handle iron at the systemic, microenvironmental, and cellular levels. Pflugers Arch. 2017;469(3-4):397-418.
31. Bellelli R, Castellone MD, Guida T, et al. NCOA4 transcriptional coactivator inhibits activation of DNA replication origins. Mol Cell. 2014;55(1):123-137.

Table 1: Iron parameters of 9-month-old wt and *Ncoa4-ko* mice fed a standard and an iron-poor diet

	Standard diet		Iron-poor diet	
	WT (n=5-10)	***Ncoa4-ko*** (n=6-13)	***WT*** (n=4)	***Ncoa4-ko*** (n=5)
TS (%)	57.21±2.58	57.60±1.80	36.70±5.03	14.10±2.88**
SI (µg/dL)	296.1±34.5	331.9±55.6	176.9±24.5	74.5±13.4*
LIC (µg iron/g dry tissue)	522.1±37.4	596.6.5±37.5	136.6±10.9	165.9±5.0
SIC (µg iron/g dry tissue)	4897±713	3518±417	1161±215	632±155
KIC (µg iron/g dry tissue)	1382±168	1276±122	748±59	772±53

TS= Transferrin Saturation; SI= Serum Iron; LIC= Liver Iron Content; SIC= Spleen Iron Content; KIC= Kidney Iron Content. Values of mean ± standard error for each group are reported. The number of animals analyzed in each group is indicated in the header. Asterisks refer to statistically significant differences between *Ncoa4-ko* and wt mice fed the same diet. *P<0.05; **P<0.01

Legend to Figures

Figure 1. Analysis of hematological parameters and erythropoiesis of wt *and Ncoa4-ko* mice fed a standard diet

Ncoa4-ko and wild-type (wt) mice (of both gender) on Sv129/J background were fed a standard diet until sacrifice when 9-month-old and complete blood count was periodically determined. In the figure are graphed: **A)** Red Blood Cells count (RBC), Hemoglobin levels (Hb), Mean Corpuscular Volume (MCV) and Mean Corpuscular Hemoglobin (MCH); **B)** Gating strategy for the analysis of erythropoiesis. Viable cells (impermeable to PI) from bone marrow and spleen were analyzed for Ter119/CD44 expression. Ter119 positive cells were gated and further analyzed with respect to FSC and CD44 surface expression for subpopulation composition. Five clusters were identified: proerythroblasts (I), basophilic erythroblasts (II), polychromatic erythroblasts (III), orthochromatic erythroblasts and immature reticulocytes (IV), and mature red cells (V)(13). Complete statistical analysis is reported in supplemental table S3; **C)** percentage of $Ter119^+$ cells on alive cells and subpopulation composition in the bone marrow (BM) and in the spleen (SP) of 3-month-old wt and *Ncoa4-ko* mice. Complete statistical analysis is reported in supplemental table S4; **D)** BFU-E and CFU-GM colony numbers generated from 10^4 bone marrow cells of 3- and 9-month-old wt and *Ncoa4-ko* mice. Mean values of 6 animals for genotype are graphed. Error bars indicate standard error. Asterisks refer to statistically significant differences between age-matched wt and *Ncoa4-ko* mice. **P*<0.05; ****P*<0.005.

Figure 2. Analysis of the iron phenotype of 9-month-old wt *and Ncoa4-ko* mice fed a standard diet

Ncoa4-ko and wild-type (wt) mice (of both gender) on Sv129/J background were fed a standard diet until sacrifice when 9-month-old. In the figure are graphed: **A)** representative pictures of Perl's staining performed on duodenal sections (thickness of section 5 µm; magnification 20X, 40X in the inset); quantitative real time PCR of **B)** Hepcidin (*Hamp*), **C)** Inhibitor of differentiation 1 (*Id1*) and **D)** Transferrin Receptor 1 (*Tfr1*) to measure mRNA

levels in the liver relative to Hypoxanthine phosphoribosyltransferase 1 (*Hprt1*); data were normalized on a wild-type mean value of 1 (RQ= relative quantification)*;* **E)** western blot and relative densitometric analysis of ferritin H (FtH) protein levels in the liver. Tubulin was used as loading control; Mean values of 6-13 animals for genotype are graphed. Error bars indicate standard error. Asterisks refer to statistically significant differences between age-matched wt and *Ncoa4-ko* mice. **P*<0.05; ***P*<0.01; ****P*<0.005.

Figure 3. Hematological parameters and erythropoiesis analysis in wt *and Ncoa4-ko* mice fed an iron-deficient diet

Ncoa4-ko and wild-type (wt) mice (of both gender) on Sv129/J background were fed an iron-deficient (ID) diet for 6 months starting at 3 months of age and complete blood count was periodically determined. In the figure are graphed: **A)** Red Blood Cells count (RBC), Hemoglobin levels (Hb), Mean Corpuscular Volume (MCV) and Mean Corpuscular Hemoglobin (MCH); **B)** percentage of $Ter119^+$ cells on alive cells and subpopulation composition (determined as described in Figure 1B) both in the bone marrow (BM) and in the spleen (SP) of 9-month-old ID wt and *Ncoa4-ko* mice. Complete statistical analysis is reported in supplemental table S5; **C)** BFU-E and CFU-GM colony numbers generated from 10^4 bone marrow cells of 9-month-old iron deficient wt and *Ncoa4-ko* mice. Mean values of 4-5 animals for genotype are graphed. Error bars indicate standard error. Asterisks refer to statistically significant differences between age-matched wt and *Ncoa4-ko* mice. **P*<0.05; ***P*<0.01; ****P*<0.005.

Figure 4. Hematological parameters, erythropoiesis and iron phenotype of *Ncoa4-ko*$^{wt\ BM}$ and *Ncoa4-ko*$^{ko\ BM}$ mice fed an iron-poor diet

Ncoa4-ko mice on Sv129/J background were transplanted with Sv129J wt (*Ncoa4-ko*$^{wt\ BM}$) or *Ncoa4-ko* (*Ncoa4-ko*$^{ko\ BM}$) bone marrow (BM). Animals were fed an iron-deficient (ID) diet for 3 months starting 2 months after BM transplantation (BMT) and complete blood count was periodically determined. In the figure are graphed: **A)** scheme of BMT procedure; **B)** Red Blood Cells count (RBC), Hemoglobin levels (Hb), Mean Corpuscular Volume (MCV) and Mean Corpuscular Hemoglobin (MCH); **C)** percentage of $Ter119^+$ cells on

alive cells and subpopulation composition (determined as described in Figure 1B) both in the bone marrow (BM) and in the spleen (SP) of *Ncoa4-ko*$^{wt\ BM}$ and *Ncoa4-ko*$^{ko\ BM}$ mice 5 months after BMT. Complete statistical analysis is reported in supplemental table S6; **D)** Spleen Iron Content (SIC), **E)** Liver Iron Content (LIC), **F)** spleen and **G)** liver Ferritin H (FtH) protein levels (representative western blot, upper panels and densitometric analysis, lower panels) using tubulin as a loading control in *Ncoa4-ko*$^{wt\ BM}$ and *Ncoa4-ko*$^{ko\ BM}$ mice 5 months after BMT. Mean values of 4-5 animals for genotype are graphed. Error bars indicate standard error. Asterisks refer to statistically significant differences between age-matched *Ncoa4-ko*$^{wt\ BM}$ and *Ncoa4-ko*$^{ko\ BM}$ mice. **P*<0.05; ***P*<0.01.

Figure 5. Erythropoiesis and iron phenotype of wt *and Ncoa4-ko* mice after an acute erythropoietin challenge

Three-month-old *Ncoa4-ko* and wild-type (wt) mice on Sv129/J background were treated with a single i.p. injection of erythropoietin (EPO, 8UI/g) or saline as control and sacrificed 15 hours later. In the figure are graphed: **A)** a scheme of the expected alterations of iron homeostasis induced by EPO injection; **B)** the percentage of Ter119^{+} alive cells and subpopulation composition (determined as described in Figure 1B) both in the bone marrow (BM) and in the spleen (SP) of EPO-treated wt and *Ncoa4-ko* mice. Complete statistical analysis is reported in supplemental table S7; **C)** real time PCR of splenic Erythroferrone (*Erfe*) to measure mRNA levels relative to Glyceraldehyde 3-Phosphate dehydrogenase (*Gapdh);* **D)** real time PCR of hepatic hepcidin *(Hamp)* to measure mRNA levels relative to Hypoxanthine phosphoribosyltransferase 1 (*Hprt1*); **E)** Transferrin Saturation and **F)** Serum Iron levels. Data in C-F are expressed as the difference (Δ) between EPO and saline (dotted grey line) treated mice of the same genotype. Mean values of 5 animals for genotype are graphed. Error bars indicate standard error. Asterisks refer to statistically significant differences between age-matched EPO-treated wt and *Ncoa4-ko* mice. **P*<0.05; ***P*<0.01; ****P*<0.005. Hashtags refer to statistically significant differences between EPO- and saline-treated mice of the same genotype. #*P*<0.05; ##*P*<0.01; ###*P*<0.005.

Figure 6. Hematological parameters of *Hbb*$^{th3/+}$ mice with germ-line deletion of *Ncoa4*

Hematological parameters of both male and female *Hbb*$^{th3/+}$ mice with wt *Ncoa4* (*Ncoa4*$^{+/+}$) or germ-line ablation of a single (*Ncoa4*$^{+/-}$) or both (*Ncoa4*$^{-/-}$) alleles were determined at 1, 2 and 4 months of age. In the figure are graphed: Red Blood Cells count (RBC), Hemoglobin levels (Hb), Mean Corpuscolar Volume (MCV) and Mean Corpuscolar Hemoglobin (MCH). Asterisks refer to statistically significant differences. ***P*<0.01; ****P*<0.005.

Figure 1

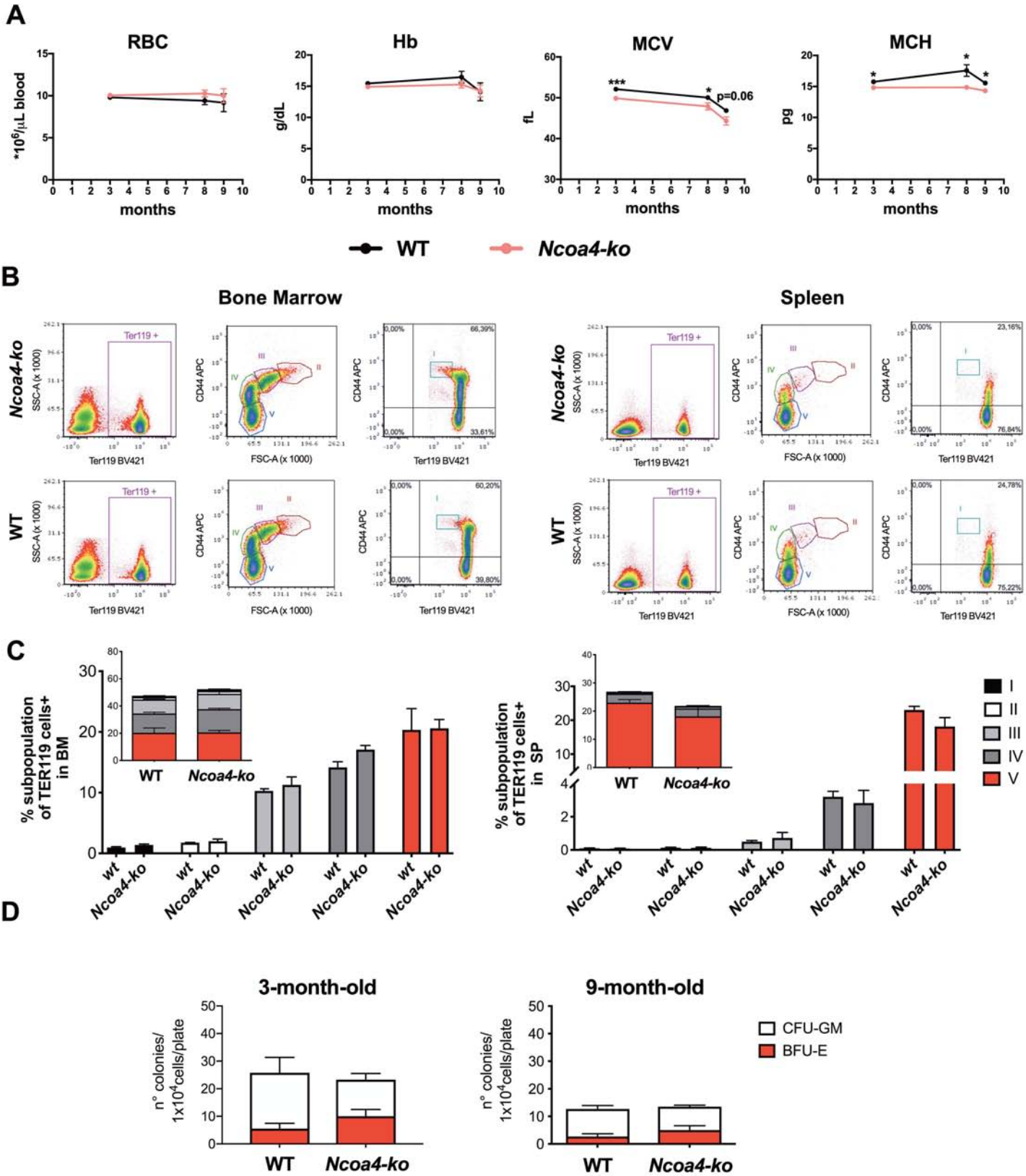
A
RBC
Hb
MCV
MCH
*10^6/μL blood
g/dL
fL
pg
months
***
*
p=0.06
WT
Ncoa4-ko
B
Bone Marrow
Spleen
Ncoa4-ko
WT
Ter119 +
SSC-A (x 1000)
Ter119 BV421
CD44 APC
FSC-A (x 1000)
66,39%
33,61%
60,20%
39,80%
23,16%
76,84%
24,78%
75,22%
C
% subpopulation of TER119 cells+ in BM
% subpopulation of TER119 cells+ in SP
WT
Ncoa4-ko
wt
I
II
III
IV
V
D
3-month-old
9-month-old
n° colonies/ 1x10^4cells/plate
CFU-GM
BFU-E

Figure 2

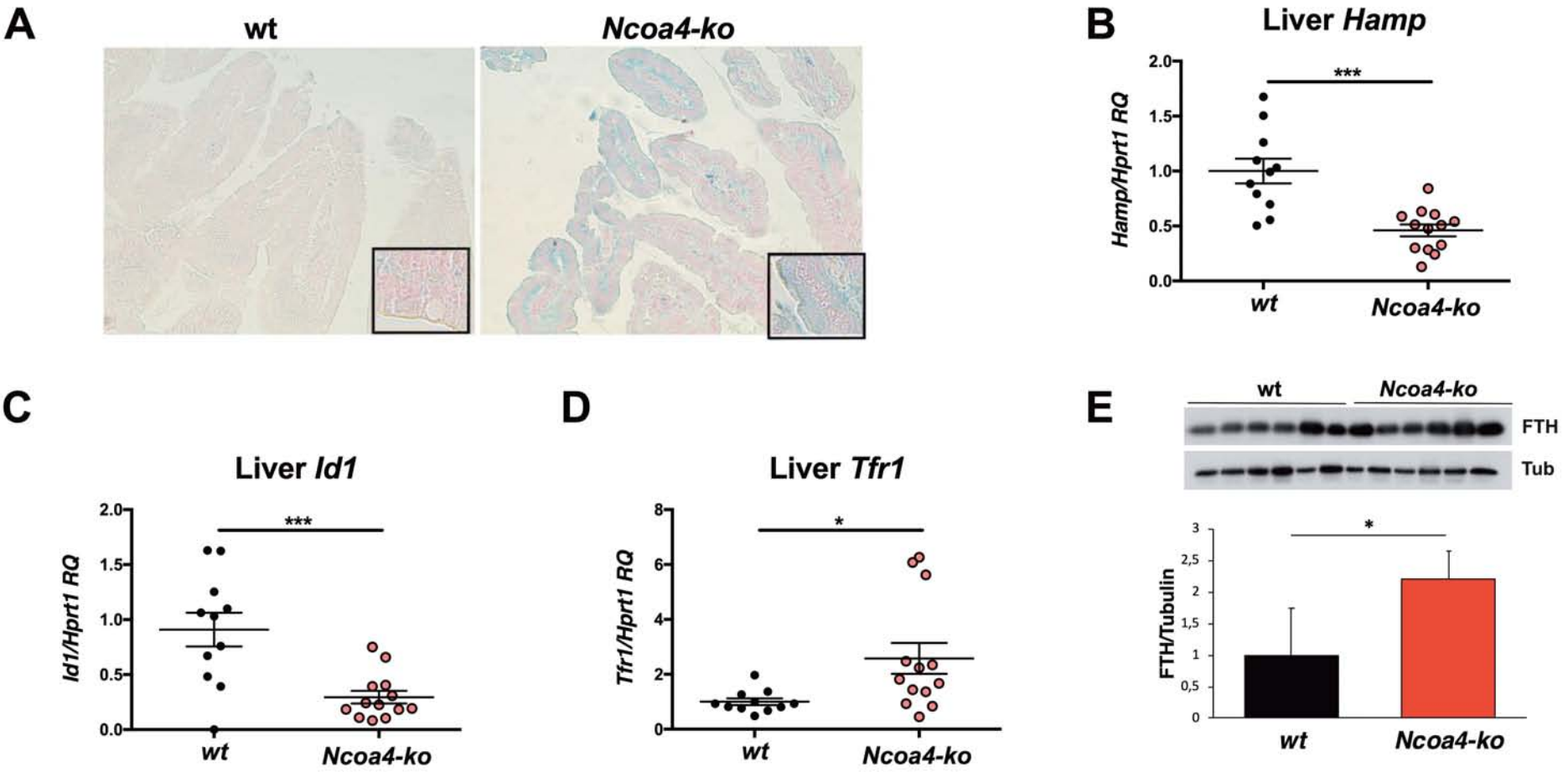
A
wt
Ncoa4-ko
B
Liver Hamp
Hamp/Hprt1 RQ
2.0
1.5
1.0
0.5
0.0
***
wt
Ncoa4-ko
C
Liver Id1
Id1/Hprt1 RQ
2.0
1.5
1.0
0.5
0.0
***
wt
Ncoa4-ko
D
Liver Tfr1
Tfr1/Hprt1 RQ
8
6
4
2
0
*
wt
Ncoa4-ko
E
wt
Ncoa4-ko
FTH
Tub
FTH/Tubulin
3
2,5
2
1,5
1
0,5
0
*
wt
Ncoa4-ko

Figure 3

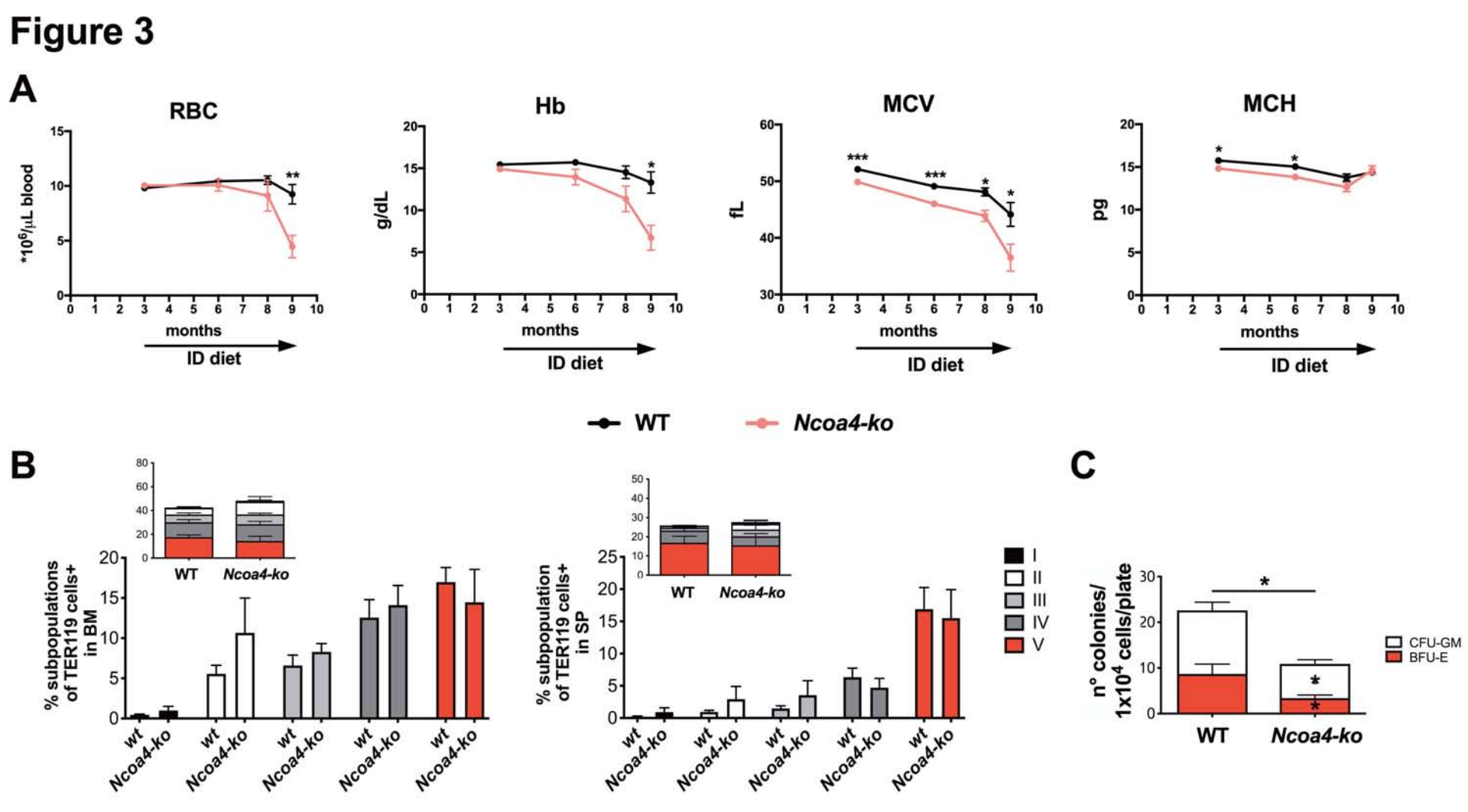
A
RBC
Hb
MCV
MCH
*10^6/µL blood
g/dL
fL
pg
months
ID diet
WT
Ncoa4-ko
B
% subpopulations of TER119 cells+ in BM
% subpopulation of TER119 cells+ in SP
I
II
III
IV
V
wt
Ncoa4-ko
C
n° colonies/ 1x10^4 cells/plate
CFU-GM
BFU-E

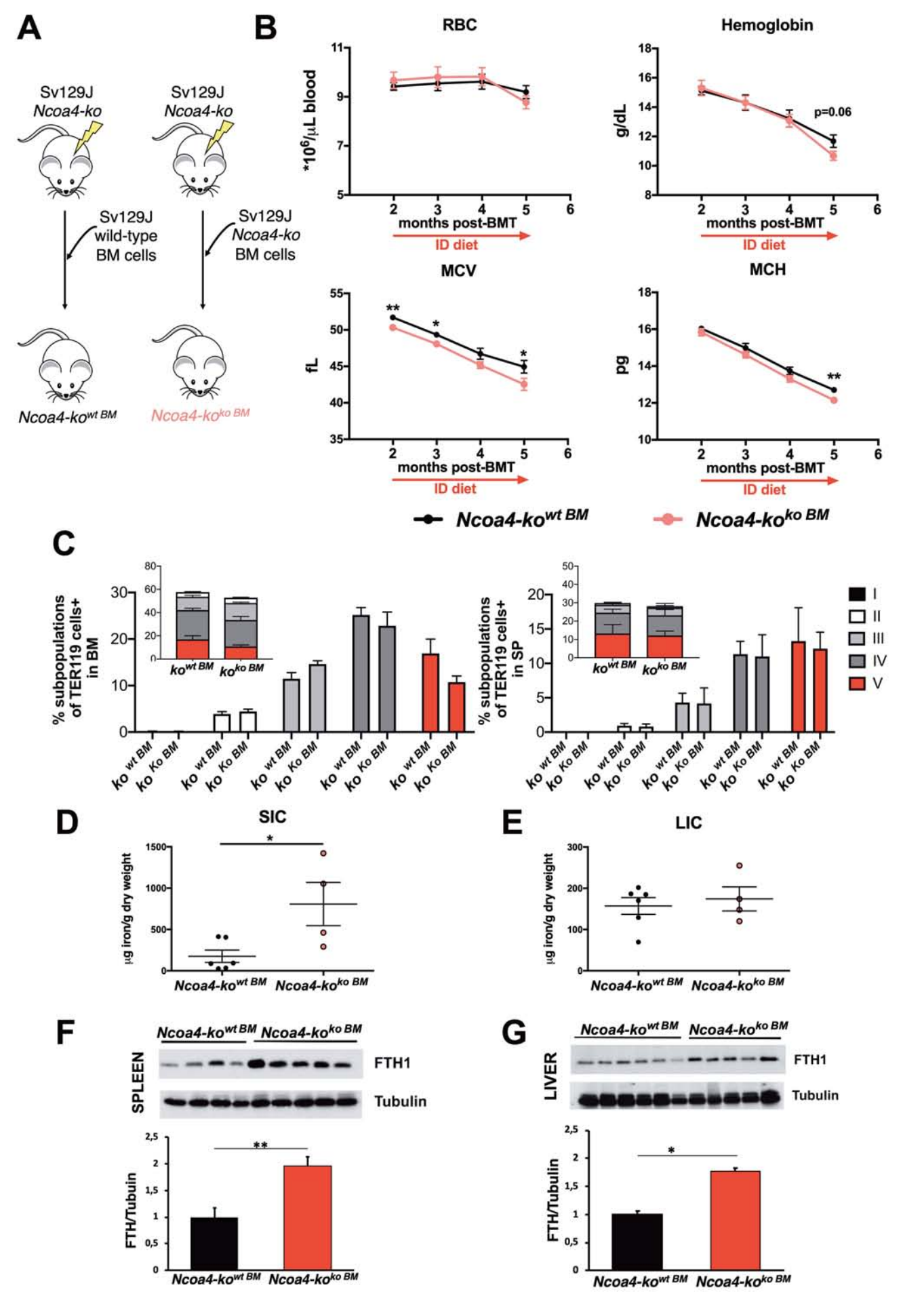
A
Sv129J
Ncoa4-ko
Sv129J
Ncoa4-ko
Sv129J
wild-type
BM cells
Sv129J
Ncoa4-ko
BM cells
Ncoa4-ko^wt BM
Ncoa4-ko^ko BM
B
RBC
*10^6/µL blood
months post-BMT
ID diet
Hemoglobin
g/dL
p=0.06
MCV
fL
MCH
pg
Ncoa4-ko^wt BM
Ncoa4-ko^ko BM
C
% subpopulations of TER119 cells+ in BM
% subpopulations of TER119 cells+ in SP
I
II
III
IV
V
D
SIC
µg iron/g dry weight
E
LIC
F
SPLEEN
FTH1
Tubulin
FTH/Tubuin
G
LIVER

Figure 5

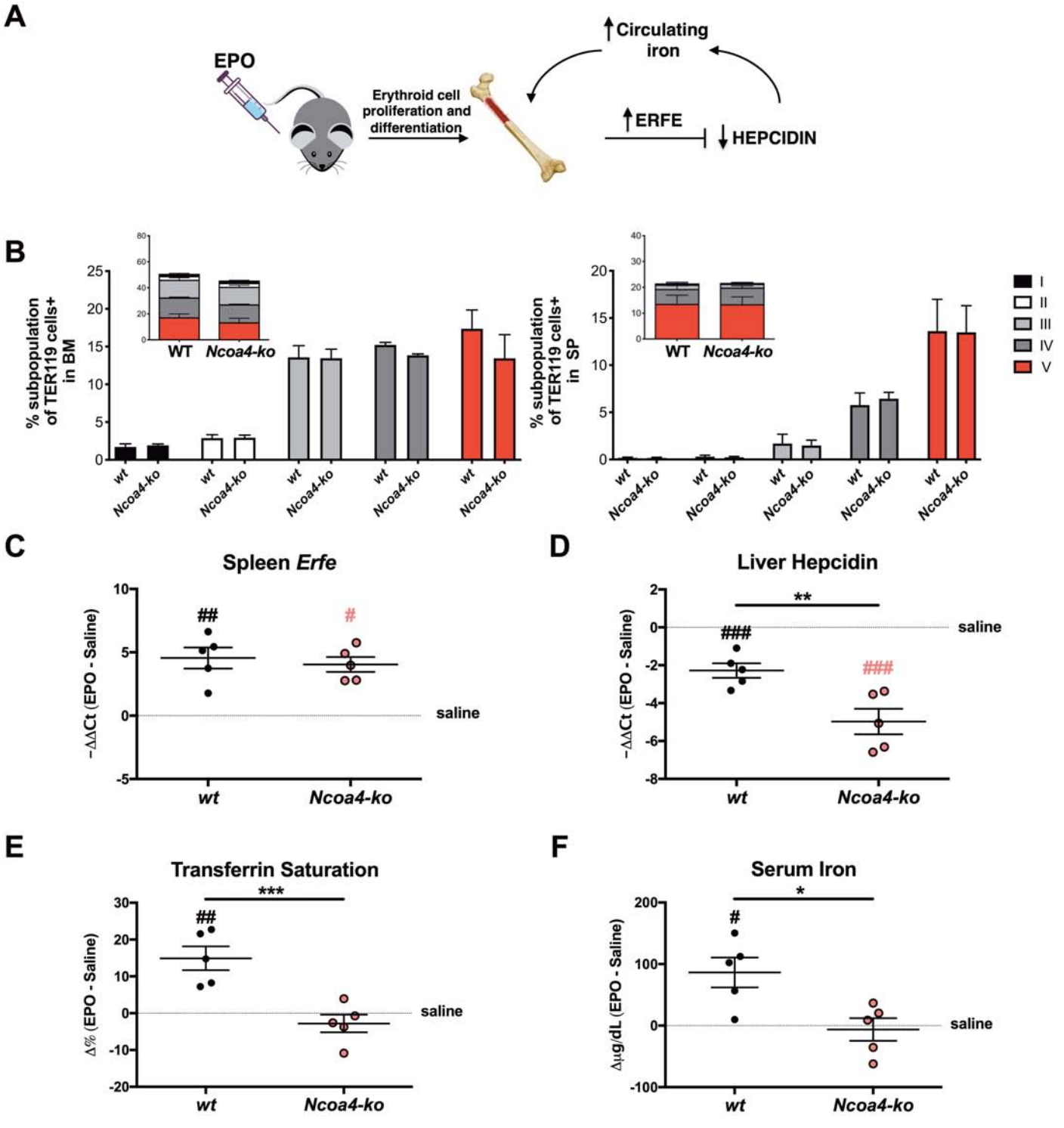
A
EPO
Erythroid cell proliferation and differentiation
Circulating iron
ERFE
HEPCIDIN
B
% subpopulation of TER119 cells+ in BM
% subpopulation of TER119 cells+ in SP
WT
Ncoa4-ko
wt
Ncoa4-ko
I
II
III
IV
V
C
Spleen Erfe
−ΔΔCt (EPO - Saline)
saline
wt
Ncoa4-ko
D
Liver Hepcidin
**
E
Transferrin Saturation
***
Δ% (EPO - Saline)
F
Serum Iron
*
Δμg/dL (EPO - Saline)

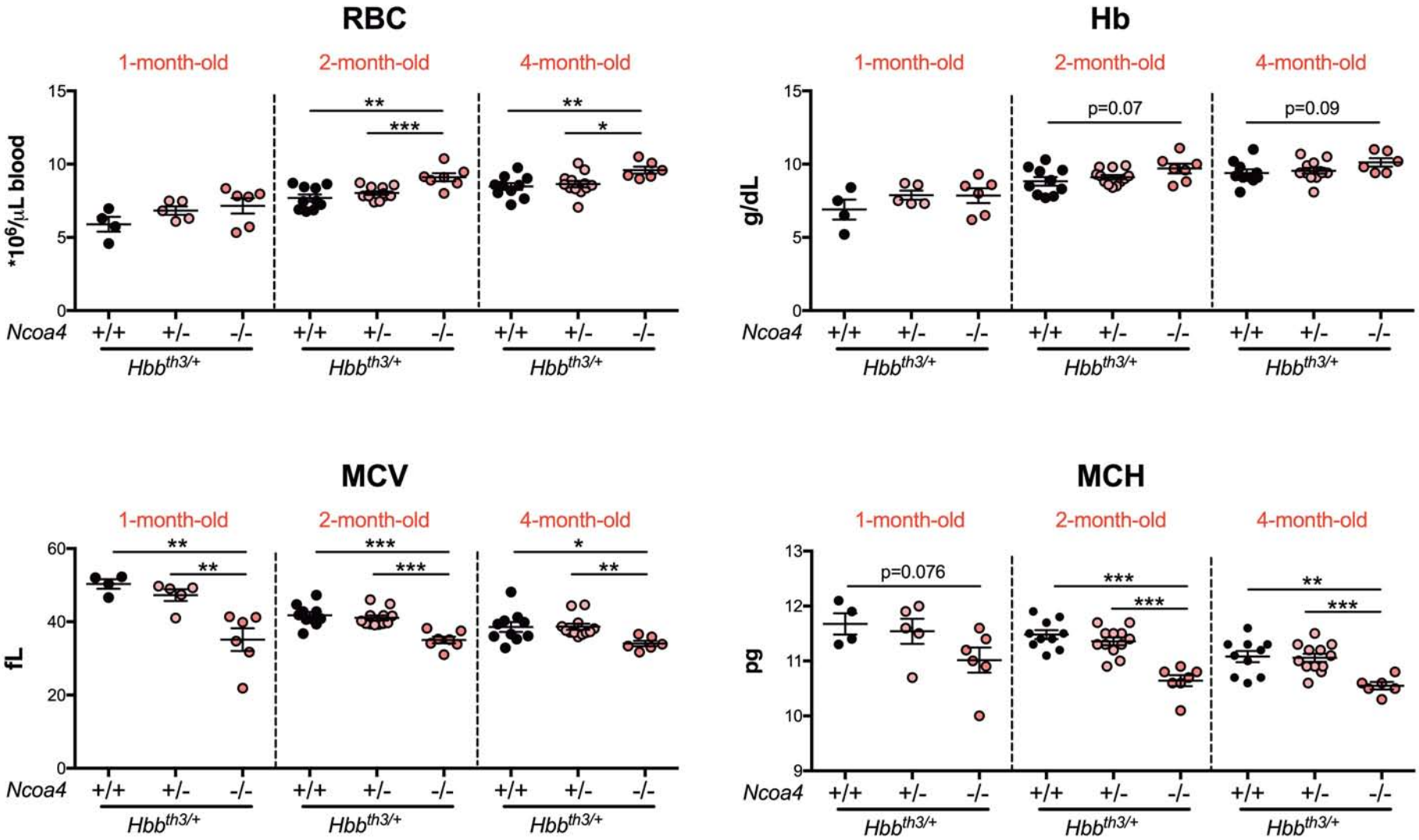
RBC
1-month-old
2-month-old
4-month-old
*10^6/μL blood
15
10
5
0
**
***
**
*
Ncoa4
+/+
+/-
-/-
Hbb^th3/+
Hb
g/dL
p=0.07
p=0.09
MCV
fL
60
40
20
0
MCH
pg
13
12
11
10
9
p=0.076

SUPPLEMENTAL MATERIAL

Supplementary methods

Sv129/J *Ncoa4-ko* mouse model generation

Several overlapping genomic clones were isolated from a λ FIX II phage library of Sv129/J mouse strain (Stratagene, Cedar Creek, TX, USA) using standard procedures. Exons II-VII of the murine *Ncoa4* gene were replaced by a neomycin-resistant (neo) cassette through homologous recombination. The targeting construct (pKO Scrambler NTKV-1906) contained the neo-cassette flanked by a BamHI-EcoRI 2800 bp fragment containing *Ncoa4* gene intron 1 sequences (left arm) and by a BamHI-KpnI 2600 bp fragment containing *Ncoa4* gene exon 8-exon 9 sequences (right arm). *Ncoa4*-pKO vector was transfected by electroporation into embryonic stem (ES) cells. Two correctly targeted ES cell lines were injected into C57BL/6 blastocysts at BIOGEM facility (Ariano Irpino, Italy). Both blastocysts gave rise to germ line chimeric animals that were then crossed to Sv129/J animals.

Bone Marrow Transplantation

BM cells were isolated from a subset of 3-month-old SV129J *Ncoa4-ko* and wt littermate male mice and $5*10^6$ cells were used for BMT in each recipient. Lethally irradiated 8-week-old *Ncoa4-ko* (Sv129/J) animals were used as recipients for the experiments reported in figure 4 and supplemental figure S5. Lethally irradiated 8-week-old C57BL/6-Ly5.1 wild-type animals were transplanted with BM cells from SV129J *Ncoa4-ko* and wt male mice for the experiments reported in supplemental figure S3.

Hematological analysis

CBC was measured on a IDEXX Procyte dx automated blood cell analyzer (Idexx Laboratories). Transferrin saturation was calculated as the ratio between serum iron and total iron binding capacity, using The Total Iron Binding Capacity Kit (Randox Laboratories Ltd.), according to the manufacturer's instructions.

Flow cytometry

Erythroid progenitors were analyzed by labeling total BM or spleen cells with rat-anti-mouse CD16/CD32 (BD Biosciences) in order to block unspecific Ig binding, and subsequently stained with BV421 rat anti-mouse Ter119 (BD Horizon, BD Biosciences) and APC rat anti-mouse CD44 (BD Pharmingen) for 30 min in the dark at 4°C. Flow cytometry analyses were performed using the FACS Canto™ II (BD Biosciences). Data were analyzed with FCS express 6 Flow (De Novo Software).

Colony-forming unit assay

Bone marrow cells from tibiae and femurs were harvested into Miltenyi Biotec buffer (autoMACS Running Buffer – MACS Separation Buffer; Miltenyi Biotec GmbH), $1*10^4$ cells were seeded in methylcellulose medium (MethoCult M3434; STEMCELL Technologies) and colonies were scored on day 10 ± 2. BFU-E were visualized by staining with benzidinehydrochloride (Sigma).

Tissue iron content

To measure total iron concentration, tissue samples were dried at 65°C for 1 week, weighed, and digested in 1 mL of acid solution (3M HCl, 0.6M trichloroacetic acid) for 20 hours at 65°C. The acid extract (20 µL) was added 1 mL of working chromogen reagent (1 volume of 0.1% bathophenanthroline sulfate and 1% thioglycolic acid solution, 5 volumes of water, and 5 volumes of saturated sodium acetate). The absorbance of the solutions was measured at 535 nm after 30 minutes of incubation at room temperature. A standard curve was generated, using an acid solution containing increasing amounts of iron sulfate.

Perl's blue staining

Formalin-fixed paraffin embedded (FFPE) sections (5 µm thickness) were deparaffinized and rehydrated by passages through xylene and alcohol series. Slides were incubated for 30 min with a solution 1:1 ferrocyanide and hydrochloric acid 2%, then washed in water

and counter stained with RED staining and mounted.

^{57}Fe solution preparation and Inductively Coupled Plasma Mass Spectrometry (ICP-MS)

The solution of the stable iron isotope ^{57}Fe was prepared dissolving ^{57}Fe (22.85g/L) into 0.4M H_2SO_4. The day of the treatment 0.83 mg of ascorbic acid and 437 mg of saccarose per mg of ^{57}Fe were added to the solution and pH was adjusted to 7 by using 1M NaOH.

^{56}Fe and ^{57}Fe isotopes content into tissue samples was determined using inductively coupled plasma mass spectrometry (ICP-MS) (Element-2; Thermo-Finnigan, Rodano (MI), Italy) at medium mass resolution (M/ΔM ~ 4,000). Sample digestion was performed by means of microwave heating for 10 min at 160 °C in 1 mL of concentrated HNO_3 (70%) (Milestone, Ethos Up Microwave Digestion System, Bergamo, Italy). A natural abundance iron standard solution was analysed during sample runs in order to check changes in the systematic bias. The calibration curve was obtained using four iron absorption standard solutions (Sigma-Aldrich) in the range 0.2–0.005 μg/mL. Natural abundance of 91.72% and 2.2% for ^{56}Fe and ^{57}Fe, respectively, were used for isotopes calibration curve calculation. For each tissue, the amount of ^{57}Fe was expressed as μg of iron per g of wet tissue. In order to measure the amount of ^{57}Fe retained by the tissue upon the treatment with ^{57}Fe-labelled solution (Figure 2), the amount of naturally occurring ^{57}Fe was subtracted from the total measured value. The amount of naturally occurring ^{57}Fe was calculated considering an average ^{57}Fe/^{56}Fe percentage of 2.4 calculated by their natural abundance. This percentage is in agreement with the values measured under basal conditions in wild-type mice.

Western-Blot

Tissues were lysed in a buffer containing 50 mM N-2-hydroxyethylpiperazine-N'-2-ethanesulfonic acid (HEPES; pH 7.5), 1% (vol/vol) Triton X-100, 150 mM NaCl, 5 mM EGTA, 50 mM NaF, 20 mM sodium pyrophosphate, 1 mM sodium vanadate, 2 mM phenylmethylsulphonyl fluoride (PMSF) and 1 μg/ml aprotinin. Lysates were clarified by centrifugation at 10,000 x g for 20 min. Lysates containing comparable amounts of proteins, estimated by a modified Bradford assay (Bio-Rad, Munchen, Germany), were subjected to direct Western blot. Immune complexes were detected with the enhanced

chemiluminescence kit (Amersham Pharmacia Biotech, Little Chalfort, UK). Immunoblotting was carried out with specific antibodies. Anti-FTH1 was from Cell Signalling Technology (Danvers, MA, USA). Anti-tubulin was from SIGMA-Aldrich. Secondary antibodies coupled to horseradish peroxidase were from Santa Cruz Biotechnology. Densitometric analysis was performed using Image Processing and Analysis in Java (Image J) program, available online.

Quantitative RT-PCR

RNA was extracted using the UPzol reagent (Biotechrabbit) for liver and spleen samples and the mini RNeasy kit (Qiagen) for BM cells. RNA (2 µg) was used for synthesis of cDNA using the High Capacity cDNA Reverse Transcription kit (Applied Biosystems), according to manufacturer's instructions. For real-time PCR analysis, specific murine Assays-on-Demand products (20x) and TaqMan Master Mix (2x) (Applied Biosystems) or specific murine oligos (designed using the Universal ProbeLibrary Assay Design Center by Roche and generated by Eurofins Italy) and SYBRgreen Master Mix (2x) (Applied Biosystems) were used. The reactions were run on 7900HT Fast Real-Time PCR System (Applied Biosystems) in a final volume of 20 or 15 µL respectively. Each cDNA sample was amplified in duplicate and the RNA level was normalized to the corresponding level of *Hprt1* or *Gapdh* mRNA. Primers used for qRT-PCR are in Supplementary Tables S1 and S2.

Supplementary tables

Table S1. Oligonucleotide primers used for qRT-PCR by TaqMan

Transcript	**Assay Id**
Hprt1	Mm01318743_m1
Hamp	Mm00519025_m1
Id1	Mm00775963_g1
Bmp6	Mm01332882_m1
Tfr1	Mm00441941_m1
Epo	Mm01202755_m1

Table S2. Oligonucleotide primers used for qRT-PCR by SybrGreen

Transcript	**Forward primer**	**Reverse primer**
Gapdh	5'-tccactcacggcaaattcaa-3'	5'-tttgatgttagtggggtctcg-3'
Erfe	5'-atggggctggagaacagc-3'	5'-tggcattgtccaagaagaca-3'
Tfr1	5'-cccaagtattctcagatatgatttca-3'	5'- cagtccagctggcaaagattat-3'
Bmp2	5'-cggactgcggtctcctaa-3'	5'-ggggaagcagcaacactaga-3'

Table S3. Complete statistical analysis relative to Figure 1C

wt *vs Ncoa4-ko*		
	BM	SP
I	0.1382	0.6702
II	0.5175	0.9081
III	0.5063	0.5369
IV	0.0648	0.6714
V	0.9474	0.1627

Table S4. Complete statistical analysis relative to Figure 1D

	wt *vs Ncoa4-ko*	
	3 months	9 months
BFU-e	p=0.2029	0.2868
CFU-GM	p=0.2914	0.3395

Table S5. Complete statistical analysis relative to Figure 3B

wt *vs Ncoa4-ko*		
	BM	SP
I	0.2834	0.2895
II	0.2435	0.2999
III	0.3629	0.3425
IV	0.6548	0.4449
V	0.5636	0.8072

Table S6. Complete statistical analysis relative to Figure 4C

$ko^{wt\ BM}$ *vs* $ko^{ko\ BM}$		
	BM	SP
I	0.9477	0.1740
II	0.5081	0.8045
III	0.1023	0.9589
IV	0.4692	0.9258
V	0.1599	0.8658

Table S7. Complete statistical analysis relative to Figure 5B

wt *vs Ncoa4-ko*		
	BM	SP
I	0.6511	0.8278
II	0.9467	0.7304
III	0.9538	0.8601
IV	0.0208	0.6690
V	0.3849	0.9773

Legend to supplementary figures

Figure S1: Erythropoietin and iron gene expression analysis in different tissues of wt *and Ncoa4-ko* mice fed a standard diet

Ncoa4-ko and wild-type (wt) mice (of both gender) on Sv129/J background were fed a standard diet until sacrifice when 9-month-old. In the figure are graphed quantitative real-time PCR to measure mRNA levels of: **A)** Erythropoietin *(Epo)* relative to Hypoxanthine phosphoribosyltransferase 1 (*Hprt1)* in the kidney; **B)** Bone Morphogenetic Protein 6 (*Bmp6*) relative to Hypoxanthine phosphoribosyltransferase 1 (*Hprt1)* and **C)** Bone Morphogenetic Protein 2 (*Bmp2*) relative to Glyceraldehyde 3-Phosphate dehydrogenase (*Gapdh)* in the liver*;* Erythroferrone *(Erfe)* in: **D)** the bone marrow (BM) and **E)** the spleen relative to Glyceraldehyde 3-Phosphate dehydrogenase (*Gapdh)**;*** **F)** Transferrin Receptor 1 *(Tfr1)* relative to Hypoxanthine phosphoribosyltransferase 1 (*Hprt1)* in the kidney. Mean values of 5-6 animals for genotype are graphed. **P*<0.05.

Figure S2: Iron phenotype and gene expression analysis in tissues of wt *and Ncoa4-ko* mice fed an iron-deficient diet

Ncoa4-ko and wild-type (wt) mice (of both gender) on Sv129/J background were fed an iron-deficient (ID) diet for 6 months starting at 3 months of age. In the figure are graphed: **A)** representative pictures of Perl's staining performed on duodenal sections (thickness of section 4 μm; magnification 20X, 40X in the inset); **B)** western blot and relative densitometric analysis of ferritin H (FtH) protein levels in the liver. Tubulin was used as loading control; quantitative real-time PCR of **C)** Hepcidin (*Hamp*), **D)** Inhibitor of differentiation 1 (*Id1*), **E)** Bone Morphogenetic Protein 6 (*Bmp6*) to measure mRNA levels relative to Hypoxanthine phosphoribosyltransferase 1 (*Hprt1*) and **F)** real-time PCR of Transferrin Receptor 1 (*Tfr1*) to measure mRNA levels relative to Glyceraldehyde 3-Phosphate dehydrogenase (*Gapdh)* in the liver***;*** **G)** real-time PCR of Transferrin Receptor 1 *(Tfr1)* and **H)** Erythropoietin *(Epo)* to measure mRNA levels relative to Hypoxanthine phosphoribosyltransferase 1 (*Hprt1)* in the kidney. Mean values of 4-5 animals for genotype are graphed. Error bars indicate standard error. Asterisks refer to statistically significant differences between age-matched wt and *Ncoa4-ko* mice. **P*<0.05; ***P*<0.01; ****P*<0.005. P<0.001.

Figure S3: Duodenal iron absorption of wt *and Ncoa4-ko* mice

Nine-month-old wt and *Ncoa4-ko* mice (of both gender) were administered a solution containing the stable iron isotope ^{57}Fe by oral gavage and sacrificed one hour later. ^{57}Fe concentration was determined via ICP-MS in **A)** duodenum, **B)** serum and **C)** liver.

Figure S4: Hematological parameters of *wt*$^{wt\ BM}$ and *wt*$^{Ncoa4\text{-}ko\ BM}$ mice fed an iron-deficient diet

C57BL/6-Ly5.1 wild-type (wt) mice were transplanted with Sv129/J wt (*wt*$^{wt\ BM}$) or *Ncoa4-ko* (*wt*$^{Ncoa4\text{-}ko\ BM}$) bone marrow (BM). Complete blood count was determined 2 months after BM transplantation. In the figure are graphed: **A)** a scheme of BMT procedures, **B)** Red Blood Cells count (RBC), **C)** Hemoglobin levels (Hb), **D)** Mean Corpuscular Volume (MCV) and **E)** Mean Corpuscular Hemoglobin (MCH). Mean values of 9-20 animals for genotype are graphed. Asterisks refer to statistically significant differences. ***P<0.005.

Figure S5: Iron phenotype of *Ncoa4-ko*$^{wt\ BM}$ and *Ncoa4-ko*$^{ko\ BM}$ mice fed an iron-poor diet

Ncoa4-ko mice on Sv129/J background were transplanted with wt (*Ncoa4-ko*$^{wt\ BM}$) or *Ncoa4-ko* (*Ncoa4-ko*$^{ko\ BM}$) bone marrow (BM). Animals were fed an iron-deficient diet for 3 months starting at 2 months after BM transplantation (BMT). In the figure are graphed: **A)** Transferrin Saturation; **B)** Serum Iron and **C)** real-time PCR to measure hepatic mRNA levels of hepcidin (*Hamp*) relative to Hypoxanthine phosphoribosyltransferase 1 (*Hprt1*) of *Ncoa4-ko*$^{wt\ BM}$ and *Ncoa4-ko*$^{ko\ BM}$ mice 5 months after BMT. Mean values of 4-5 animals for genotype are graphed.

Figure S6: Gene expression analysis of wt *and Ncoa4-ko* mice after an acute erythropoietin challenge

Three-month-old *Ncoa4-ko* and wild-type (wt) mice on Sv129/J background were treated with a single i.p. injection of erythropoietin (EPO, 8UI/g) or saline as a control and sacrificed 15 hours later. In the figure are graphed **A)** percentage of Ter119^{+} cells on alive cells and subpopulation composition (determined as in Figure 1) both in the bone marrow (BM) and in the spleen (SP) of saline (data from Figure 1B) and EPO (data from Figure 4B) treated mice; real-time PCR for **B)** Inhibitor of differentiation 1 (*Id1*), **C)** Bone Morphogenetic Protein 6 (*Bmp6*) and **D)** Bone Morphogenetic Protein 2 (*Bmp2*) to measure mRNA levels relative to Hypoxanthine phosphoribosyltransferase 1 (*Hprt1*) in the

liver. Real-time data are expressed as the difference (Δ) between EPO and saline (dotted grey line) treated mice of the same genotype. Mean values of 5 animals for genotype are graphed. Error bars indicate standard error. Asterisks refer to statistically significant differences between age-matched EPO-treated wt and *Ncoa4-ko* mice. ***P*<0.01. Hashtag refers to statistically significant differences between EPO- and saline-treated mice of the same genotype. #*P*<0.05.

Supplemental Figures

Figure S1

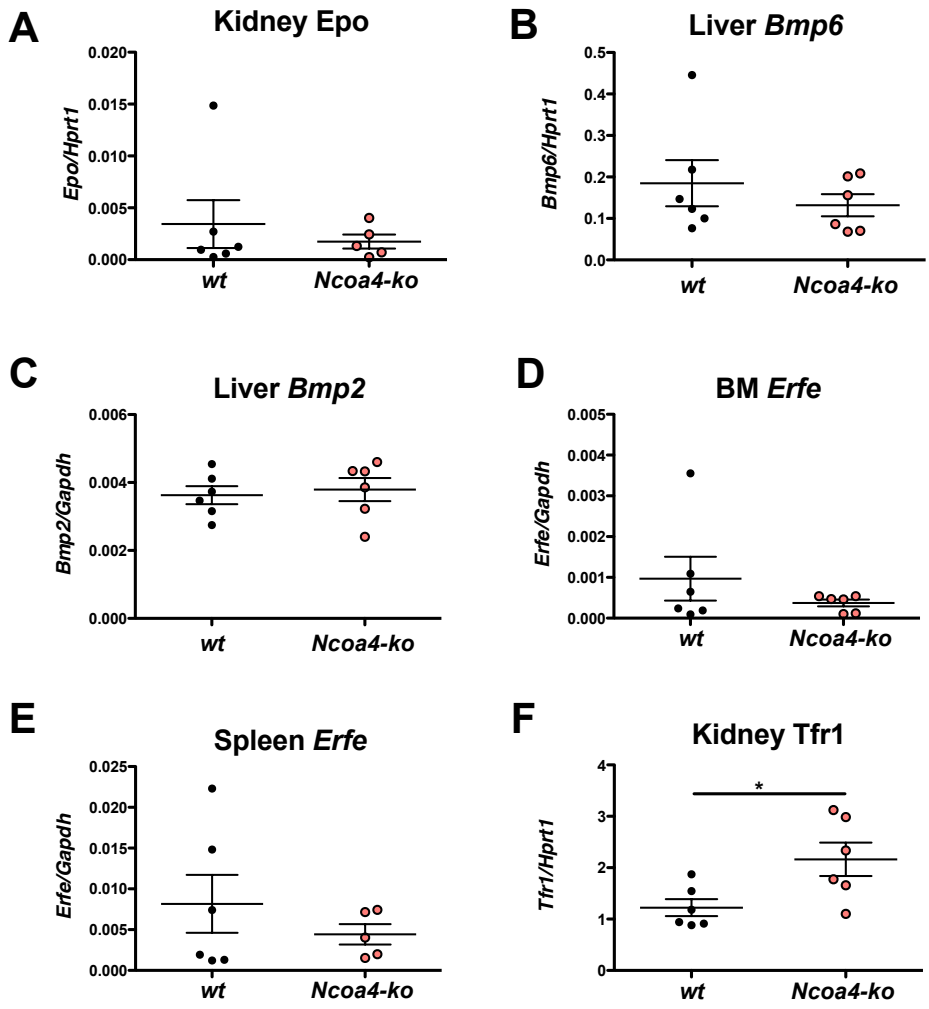

Figure S2

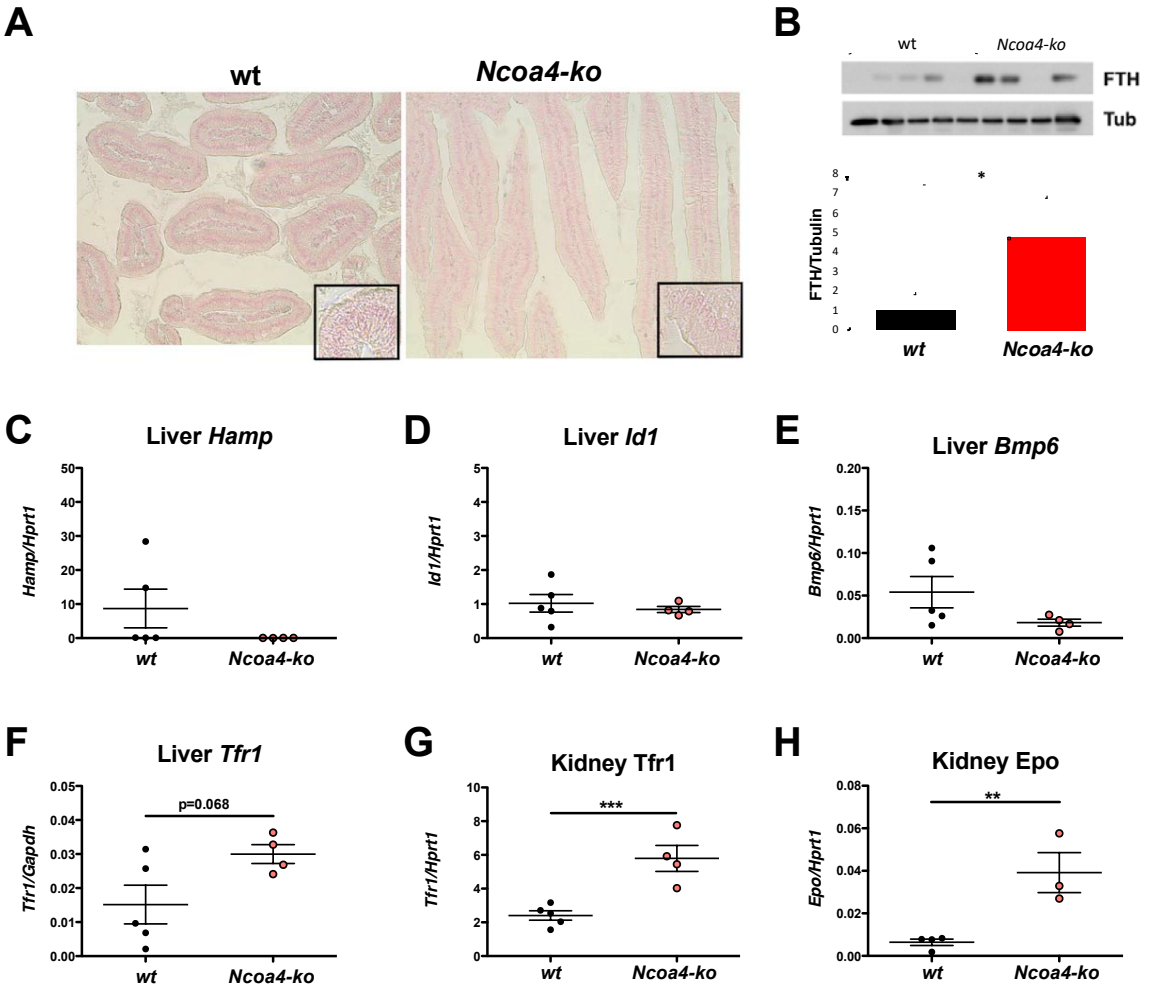

Figure S3

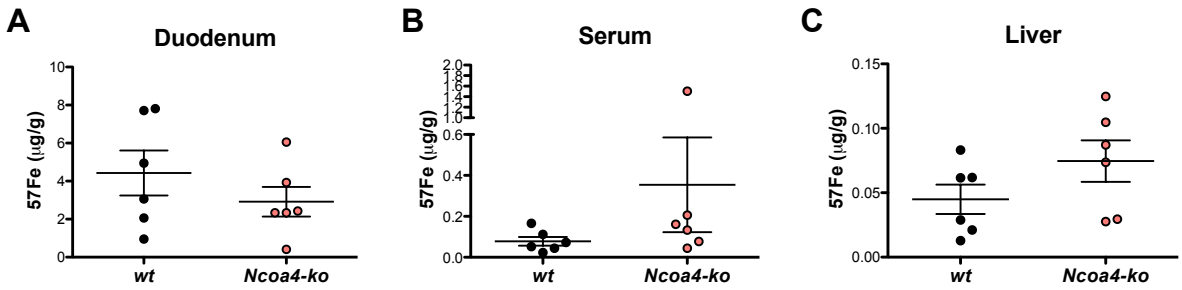

Figure S4

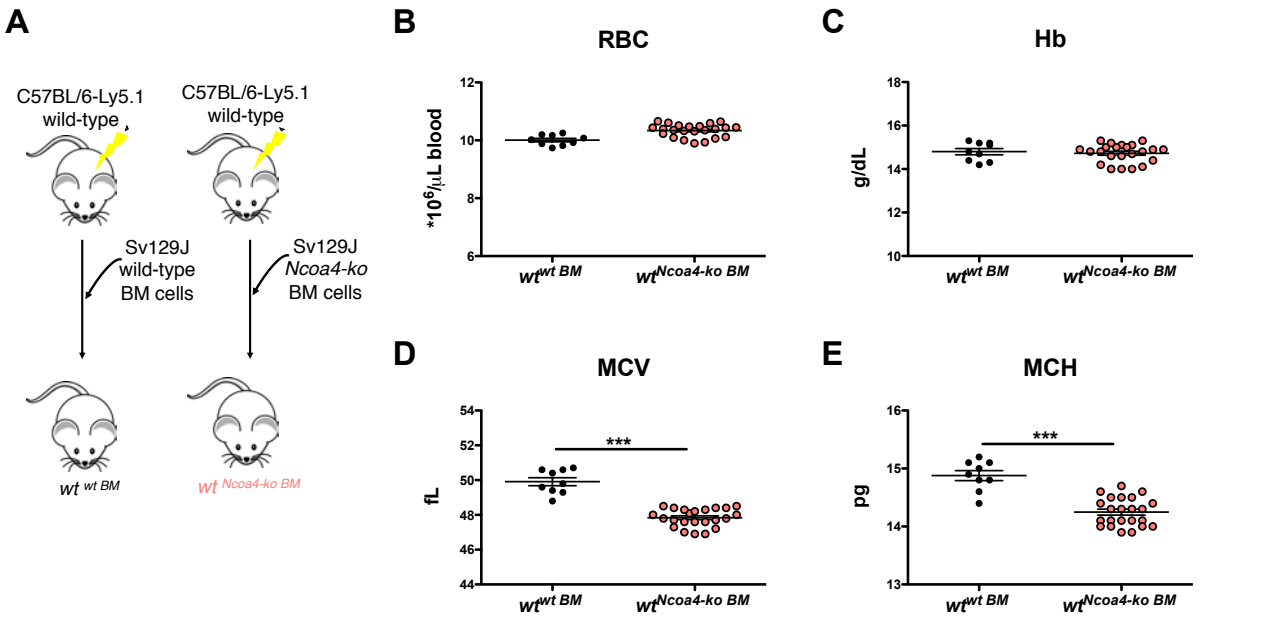
A
C57BL/6-Ly5.1 wild-type
C57BL/6-Ly5.1 wild-type
Sv129J wild-type BM cells
Sv129J Ncoa4-ko BM cells
wt wt BM
wt Ncoa4-ko BM
B
RBC
*10^6/µL blood
wtwt BM
wtNcoa4-ko BM
C
Hb
g/dL
wtwt BM
wtNcoa4-ko BM
D
MCV
fL
***
wtwt BM
wtNcoa4-ko BM
E
MCH
pg
***
wtwt BM
wtNcoa4-ko BM

Figure S5

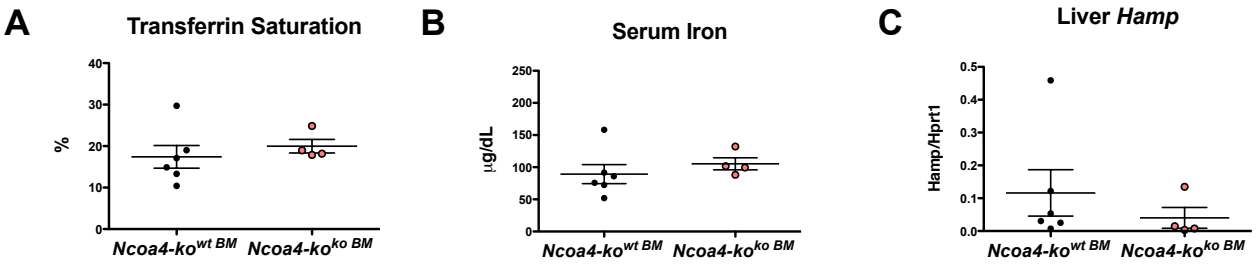
A
Transferrin Saturation
%
Ncoa4-kowt BM
Ncoa4-koko BM
B
Serum Iron
µg/dL
Ncoa4-kowt BM
Ncoa4-koko BM
C
Liver Hamp
Hamp/Hprt1
Ncoa4-kowt BM
Ncoa4-koko BM

Figure S6

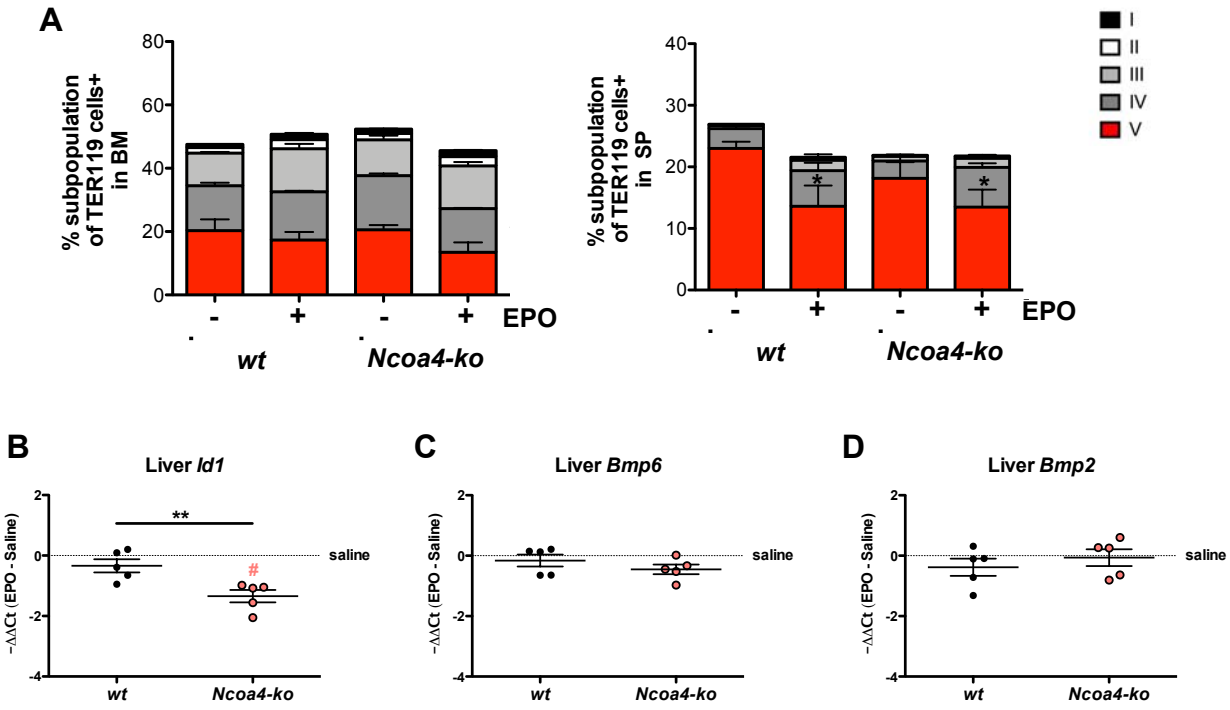
A
% subpopulation of TER119 cells+ in BM
80
60
40
20
0
- + - + EPO
wt
Ncoa4-ko
% subpopulation of TER119 cells+ in SP
40
30
20
10
0
- + - + EPO
wt
Ncoa4-ko
I
II
III
IV
V
B
Liver Id1
**
#
saline
-ΔΔCt (EPO - Saline)
2
0
-2
-4
wt
Ncoa4-ko
C
Liver Bmp6
saline
-ΔΔCt (EPO - Saline)
wt
Ncoa4-ko
D
Liver Bmp2
saline
-ΔΔCt (EPO - Saline)
wt
Ncoa4-ko